Structural Analysis of Axisymmetric Solids

EDWARD L. WILSON*
Aerojet-General Corporation, Sacramento, Calif.

The finite element method is applied to the determination of stresses and displacements in axisymmetric solids of arbitrary geometry subjected to thermal or mechanical loads. Complex structures with anisotropic material properties are included in the formulation. The structure is replaced by a system of elements interconnected along circumferential joints or nodal circles. Based on energy principles, equilibrium equations for the complete structure are formed. In the case of axisymmetric loading, the radial and axial displacements at the nodal circles are the unknowns of the system. For nonaxisymmetric loads, the three displacements at each nodal circle are expanded in Fourier series. By recognizing the orthogonality properties of the trigonometric functions, the analysis is divided into a sum of a series of two-dimensional analyses. In this investigation, the preceding procedure is used as the basis for the development of computer programs for the stress analysis of axisymmetric solids. Examples are presented to demonstrate the validity and practicality of the method.

I. Introduction

IN the aerospace industry, the stress analysis of complex axisymmetric structures of arbitrary shape subjected to thermal and mechanical loads is of considerable interest. Rocket nozzles and cases, solid-propellant grains, and spacecraft heat shields are practical examples of such structures. Although the governing differential equations for solids of revolution have been known for many years, closed form solutions have been obtained for only a limited number of structures; thus, the stress analyst must rely on experimental or numerical techniques. The finite difference method has been the most popular of the numerical techniques; however, for structures of composite materials and of arbitrary geometry, this procedure is difficult to apply.

In the present investigation, the finite element idealization is used as the basic numerical procedure. This technique has been applied successfully in the stress analysis of many complex structures.[1-3] In Ref. 4 impressive results were obtained in the analysis of axisymmetric shells approximated by a series of truncated cone elements. The approach, which is presented here, is similar in many respects to existing methods used in the analysis of two-dimensional stress problems.[5-7] Recently, the finite element method was applied to the structural analysis of axisymmetric solids subjected to axisymmetric loads.[8] In the present paper, the finite element method is used in the determination of stresses and displacements developed within elastic solids of revolution which are subjected to axisymmetric or nonaxisymmetric loads. Emphasis is placed on the application of the technique to complex aerospace structures.

II. Method of Analysis

The term finite element indicates the type of idealization, which is used to reduce the continuous structure to a system of discrete bodies. The redundant force or flexibility method may be applied for the solution of a system of finite elements; however, if an automated digital computer program is to be produced, the displacements and internal stresses of the system are generally determined by the direct stiffness method, since this approach is most readily programed.

In the finite element approximation of axisymmetric solids, the continuous structure is replaced by a system of axisymmetric elements, which are interconnected at circumferential joints or nodal circles. Figure 1 illustrates a finite element idealization of a typical axisymmetric solid. Equilibrium equations, in terms of unknown nodal circle displacements, are developed at each nodal circle. A solution of this set of equations constitutes a solution to the system.

The advantages of the finite element method, as compared to other numerical approaches, are numerous. The method is completely general with respect to geometry and material properties. Complex bodies composed of many different materials are easily represented. Since anisotropic materials are automatically included in the formulation, filament structures are readily handled. Displacement or stress boundary conditions may be specified at any nodal circle within the finite element system. Arbitrary thermal, mechanical, and accelerational loads are possible. Mathematically, it can be shown that the method converges to the exact solution as the number of elements is increased[9]; therefore, any desired degree of accuracy may be obtained. In addition, the finite element approach generates equilibrium equations, which produce a symmetric, positive-definite matrix, which may be placed in a band form and solved with a minimum of computer storage and time.

A. Equilibrium Equations for an Arbitrary Finite Element System

The first step in the determination of an expression for nodal circle forces in terms of nodal circle displacements for

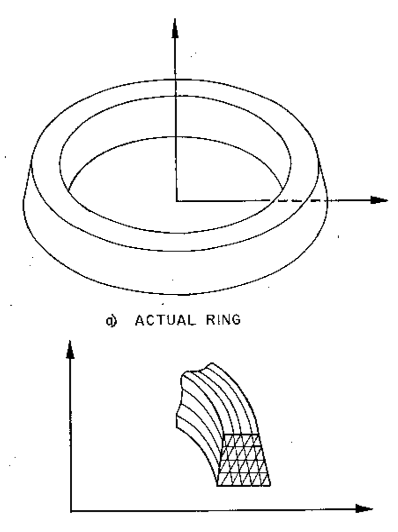

Fig. 1 Finite element idealization.

Presented as Preprint 64-143 at the AIAA 2nd Aerospace Sciences Meeting, New York, N. Y., January 25–27, 1965; revision received August 2, 1965.

* Senior Research Engineer, Solid Rocket Operations. Associate Fellow Member.

a finite element system is to assume a form for the displacement field within each element. It is necessary that this displacement field satisfies compatibility between elements of the system. Based on this approximation, an expression for the displacements $[u^m]$ within a typical element m in terms of the nodal circle displacements $[u]$ is developed.

$$[u^m] = [d^m][u] \tag{1}$$

Also, the strains $[\epsilon^m]$ within the element are expressed in terms of nodal circle displacements.

$$[\epsilon^m] = [a^m][u] \tag{2}$$

The column matrix $[u]$ contains all of the possible nodal circle displacements; therefore, the matrices $[d^m]$ and $[a^m]$ contain mostly zero elements.

For an elastic material, the stresses at any point within the element are expressed in terms of the corresponding strains and thermal effects by the elastic stress-strain relationship. Or in matrix form

$$[\sigma^m] = [C^m][\epsilon^m] - [\tau^m] \tag{3}$$

From a consideration of energy principles,[8] the force equilibrium of a system of finite elements is written as

$$[Q] = [K][u] \tag{4}$$

The stiffness matrix for a complete system of M finite elements is given by the summation of element stiffnesses

$$[K] = \sum_{m=1}^{M} [k^m] \tag{5}$$

and the load matrix is given by

$$[Q] = [S] + \sum_{m=1}^{M} [L^m] \tag{6}$$

where [S] is a matrix of concentrated nodal circle loads, which are applied externally. The element stiffness matrix is defined as

$$[k^m] = \int_{\text{vol}} [a^m]^T[C^m][a^m]\, dV \tag{7}$$

and the element load matrix is given by

$$[b^m] = \int_{\text{vol}} \{[d^m]^T[F^m] + [a^m]^T[\tau^m]\}\, dV + \int_{\text{area}} [d^m]^T[P^m]\, dS \tag{8a}$$

where $[F^m]$ is a matrix of body force components, and $[P^m]$ is a matrix of surface tractions. The surface integral exists only if the mth element is on a loaded boundary of the structure. For the purpose of simplicity, the present paper will be concerned with only thermal loads; therefore, Eq. (8a) may be rewritten as

$$[L^m] = \int [a^m]^T[\tau^m] \cdot dV \tag{8b}$$

B. Boundary Conditions

Equation (4) represents the relationship between all of the nodal circle forces and all of the nodal circle displacements. Mixed boundary conditions are considered by rewriting Eq. (4) in the following partitioned form:

$$\begin{bmatrix} Q_a \\ \hline Q_b \end{bmatrix} = \begin{bmatrix} K_{aa} & \vdots & K_{ab} \\ \hline K_{ba} & \vdots & K_{bb} \end{bmatrix} \begin{bmatrix} u_a \\ \hline u_b \end{bmatrix} \tag{9}$$

where $[Q_a]$ is the specified nodal point forces, $[Q_b]$ is the unknown nodal point forces, $[u_a]$ is the unknown nodal point displacements, and $[u_b]$ is the specified nodal point displacements. The first part of Eq. (9) may be written as a separate matrix equation

$$[Q_a] = [K_{aa}][u_a] + [K_{ab}][u_b] \tag{10}$$

and then expressed in the following reduced form:

$$[Q^*] = [K_{aa}][u_a] \tag{11}$$

where the modified load vector is given by

$$[Q^*] = [Q_a] - [K_{ab}][u_b] \tag{12}$$

After Eq. (11) is solved for the nodal point displacements, the strains within any element in the system are evaluated by the direct application of Eq. (2). The corresponding stresses are calculated from the stress-strain relationship, Eq. (3).

III. Element Stiffnesses

Several types of elements may be used in the representation of a structure. Although a ring with a triangular cross section is the most versatile, for purposes of automatic mesh generation, a quadrilateral element is often desirable. A truncated cone element is useful in the approximation of the flanges of sandwich type structures. For convenience, the superscript m, which denoted a typical element in the previous section, will be omitted in the remaining development.

A. Triangular Ring Element: Axisymmetric Load

The cross section of a typical triangular ring element is shown in Fig. 2. The displacements in the r-z plane within the element are assumed to be of the following form:

$$u_r(r, z) = b_1 + b_2 r + b_3 z \tag{13a}$$

$$u_z(r, z) = b_4 + b_5 r + b_6 z \tag{13b}$$

This linear displacement field assures continuity between elements, since "lines, which are initially straight, remain straight in their displaced position."

If Eqs. (13a) and (13b) are evaluated at the three vertices of the triangular ring element, the following matrix equation is obtained:

$$\begin{bmatrix} u_r^i & u_z^i \\ u_r^j & u_z^j \\ u_r^k & u_z^k \end{bmatrix} = \begin{bmatrix} 1 & r_i & z_i \\ 1 & r_j & z_j \\ 1 & r_k & z_k \end{bmatrix} \begin{bmatrix} b_1 & b_4 \\ b_2 & b_5 \\ b_3 & b_6 \end{bmatrix} \tag{14}$$

A solution of Eq. (14) yields the following expression for the constants b_i in terms of the displacement at the vertices:

$$\begin{bmatrix} b_1 & b_4 \\ b_2 & b_5 \\ b_3 & b_6 \end{bmatrix} = [D] \begin{bmatrix} u_r^i & u_z^i \\ u_r^j & u_z^j \\ u_r^k & u_z^k \end{bmatrix} \tag{15a}$$

where

$$[D] = \frac{1}{\lambda} \begin{bmatrix} r_j z_k - r_k z_j & r_k z_i - r_i z_k & r_i z_j - r_j z_i \\ z_j - z_k & z_k - z_i & z_i - z_j \\ r_k - r_j & r_i - r_k & r_j - r_i \end{bmatrix} \tag{15b}$$

in which

$$\lambda = r_j(z_k - z_i) + r_i(z_j - z_k) + r_k(z_i - z_j)$$

Equation (15a) may be written in an expanded form where the constants and displacements are column matrices:

$$[b] = [h][u] \tag{16}$$

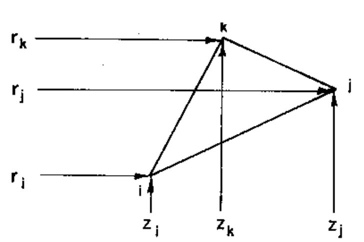

Fig. 2 Triangular element.

The strains within the element are obtained from Eqs. (13a) and (13b), thus

$$\epsilon_{rr} = \partial u_r/\partial r = b_2 \qquad \epsilon_{zz} = \partial u_z/\partial z = b_6$$

$$\epsilon_{\theta\theta} = u_r/r = (1/r)b_1 + b_2 + (z/r)b_3$$

$$\epsilon_{rz} = (\partial u_r/\partial z) + (\partial u_z/\partial r) = b_3 + b_5$$

which may be written in matrix form as

$$\begin{bmatrix} \epsilon_{rr} \\ \epsilon_{zz} \\ \\ \epsilon_{\theta\theta} \\ \epsilon_{rz} \end{bmatrix} = \begin{bmatrix} 0 & 1 & 0 & 0 & 0 & 0 \\ 0 & 0 & 0 & 0 & 0 & 1 \\ 1/r & 1 & z/r & 0 & 0 & 0 \\ 0 & 0 & 1 & 0 & 1 & 0 \end{bmatrix} \begin{bmatrix} b_1 \\ b_2 \\ b_3 \\ b_4 \\ b_5 \\ b_6 \end{bmatrix} \tag{17a}$$

or symbolically

$$[\epsilon] = [g][b] \tag{17b}$$

The substitution of Eq. (16) into Eq. (17) yields

$$[\epsilon] = [g][h][u]$$

Thus, the strain-displacement transformation matrix, as defined in Eq. (2), is

$$[a] = [g][h] \tag{18}$$

With this definition of $[a]$, the element stiffness matrix, Eq. (7), is rewritten as

$$[k] = \int [h]^T[g]^T[C][g][h]\cdot dV \tag{19}$$

Since $[h]$ is not a function of space, Eq. (19) becomes

$$[k] = [h]^T\{\int[g]^T[C][g]\cdot dV\}[h] \tag{20}$$

and the thermal load matrix, Eq. (8b), reduces to

$$[L] = [h]^T\{\int[g]^T[\tau]\cdot dV\} \tag{21}$$

For most axisymmetric structures, the following anisotropic stress-strain relationship is sufficiently general:

$$\begin{bmatrix} \sigma_{rr} \\ \sigma_{zz} \\ \sigma_{\theta\theta} \\ \sigma_{rz} \end{bmatrix} = \begin{bmatrix} C_{11} & C_{12} & C_{13} & 0 \\ C_{12} & C_{22} & C_{23} & 0 \\ C_{13} & C_{23} & C_{33} & 0 \\ 0 & 0 & 0 & C_{44} \end{bmatrix} \begin{bmatrix} \epsilon_{rr} \\ \epsilon_{zz} \\ \epsilon_{\theta\theta} \\ \epsilon_{rz} \end{bmatrix} - \begin{bmatrix} \tau_1 \\ \tau_2 \\ \tau_3 \\ 0 \end{bmatrix} \tag{22}$$

where

$$\tau_1 = T(C_{11}\,\alpha_r + C_{12}\,\alpha_z + C_{13}\,\alpha_\theta)$$

$$\tau_2 = T(C_{12}\,\alpha_r + C_{22}\,\alpha_z + C_{23}\,\alpha_\theta)$$

$$\tau_3 = T(C_{13}\,\alpha_r + C_{23}\,\alpha_z + C_{33}\,\alpha_\theta)$$

and α_r, α_z, and α_θ are the coefficients of thermal expansions in the r, z, and θ directions, respectively. For this type of material, the terms under the integral in Eqs. (20) and (21) are

$$[g]^T[C][g] =$$

$$\begin{bmatrix} (1/r^2)C_{33} & (1/r)(C_{13} + C_{33}) & (z/r^2)C_{33} & 0 & 0 & (1/r)C_{23} \\ (1/r)(C_{13} + C_{33}) & C_{11} + 2C_{13} + C_{13} & (z/r)(C_{13} + C_{33}) & 0 & 0 & C_{12} + C_{23} \\ (z/r^2)C_{33} & (z/r)(C_{13} + C_{33}) & (z^2/r^2)C_{33} + C_{44} & 0 & C_{44} & (z/r)C_{23} \\ 0 & 0 & 0 & 0 & & 0 \\ 0 & 0 & C_{44} & 0 & C_{44} & 0 \\ (1/r)C_{23} & C_{12} + C_{23} & (z/r)C_{23} & 0 & 0 & C_{22} \end{bmatrix} \tag{23}$$

and

$$[G]^T[\tau] = \begin{bmatrix} (1/r)\tau_3 \\ \tau_1 + \tau_3 \\ (z/r)\tau_3 \\ 0 \\ 0 \\ \tau_2 \end{bmatrix} \tag{24}$$

Equations (23) and (24) may be coded directly, since the integrals over the volume of the element for the various functions are most conveniently evaluated numerically within a computer program. The singularity at $r = 0$ is handled by setting the radius of the nodal circles at the axis of symmetry to a small finite valve; then, the boundary condition of zero radial displacement is enforced. The element stiffness matrix, Eq. (20), and the thermal load matrix, Eq. (21), are then formed by standard matrix operations.

B. Triangular Ring Element Nonaxisymmetric Load

In this section a theory is presented for the analysis of solids of revolution subjected to nonaxisymmetric loads, which are symmetric about a plane containing the axis of revolution. The method involves the expansion of the temperature distribution, nodal circle forces and nodal circle displacement in Fourier series.

$$T = \Sigma\, T_n\,(r, z)\cos n\theta \tag{25a}$$

$$S_r = \Sigma\, S_{rn}\,(r, z)\cos n\theta \tag{25b}$$

$$S_z = \Sigma\, S_{zn}\,(r, z)\cos n\theta \tag{25c}$$

$$S_\theta = \Sigma\, S_{\theta n}\,(r, z)\sin n\theta \tag{25d}$$

$$u_r = \Sigma\, u_{rn}\,(r, z)\cos n\theta \tag{25e}$$

$$u_z = \Sigma\, u_{zn}\,(r, z)\cos n\theta \tag{25f}$$

$$u_\theta = \Sigma\, u_{\theta n}\,(r, z)\sin n\theta \tag{25g}$$

By making use of the orthogonality properties of the harmonic functions, the three-dimensional analysis is divided into a series of uncoupled two-dimensional analyses in which the displacement amplitudes u_n are the unknowns. For a typical harmonic n, Eq. (7) and (8) are rewritten as

$$[k_n] = [h]^T\{\int[g_n]^T[C][g_n]dV\}\;[h] \tag{26a}$$

$$[L_n] = [h]^T\{\int[g_n]^T[\tau_n]\,dV\} \tag{26b}$$

Within each element, the displacements are assumed to be linear functions in the r-z plane, or

$$u_r = \Sigma\,(b_{1n} + b_{2n}\,r + b_{3n}\,z)\cos n\theta \tag{27a}$$

$$u_z = \Sigma\,(b_{4n} + b_{5n}\,r + b_{6n}\,z)\cos n\theta \tag{27b}$$

$$u_\theta = \Sigma\,(b_{7n} + b_{8n}\,r + b_{9n}\,z)\sin n\theta \tag{27c}$$

The strains, which correspond to these displacements, are

$$\epsilon_{rr} = \Sigma\,\epsilon_{rrn}\cos n\theta = \partial u_r/\partial r \tag{28a}$$

$$\epsilon_{zz} = \Sigma\,\epsilon_{zzn}\cos n\theta = \partial u_z/\partial z \tag{28b}$$

$$\epsilon_{\theta\theta} = \Sigma\,\epsilon_{\theta\theta n}\cos n\theta = (1/r)(\partial u_\theta/\partial\theta) + (u_r/r) \tag{28c}$$

$$\epsilon_{rz} = \Sigma\,\epsilon_{rzn}\cos n\theta = (\partial u_r/\partial z) + (\partial u_z/\partial r) \tag{28d}$$

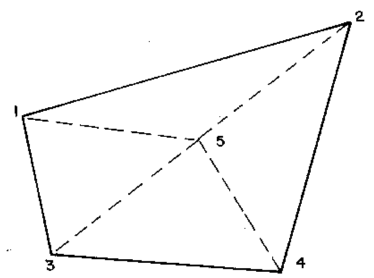

Fig. 3 Quadrilateral element.

$$\epsilon_{r\theta} = \Sigma\, \epsilon_{r\theta n} \sin n\theta = (1/r)(\partial u_r/\partial\theta) + (\partial u_\theta/\partial r) - (u_\theta/r) \tag{28e}$$

$$\epsilon_{z\theta} = \Sigma\, \epsilon_{z\theta n} \sin n\theta = (\partial u_\theta/\partial z) + (1/r)(\partial u_z/\partial\theta) \tag{28f}$$

From these equations, the strain amplitudes ϵ_{ijn} are obtained from the assumed displacements, Eqs. (27), and are written in the following form:

$$\begin{bmatrix} \epsilon_{rrn} \\ \epsilon_{zzn} \\ \epsilon_{\theta\theta n} \\ \epsilon_{rzn} \\ \epsilon_{r\theta n} \\ \epsilon_{z\theta n} \end{bmatrix} = \begin{bmatrix} 0 & 1 & 0 & 0 & 0 & 0 & 0 & 0 & 0 \\ 0 & 0 & 0 & 0 & 0 & 1 & 0 & 0 & 0 \\ 1/r & 1 & z/r & 0 & 0 & 0 & n/r & n & (nz/r) \\ 0 & 0 & 1 & 0 & 1 & 0 & 0 & 0 & 0 \\ -(n/r) & -n & -(nz/r) & 0 & 0 & 0 & -(1/r) & 0 & -(z/r) \\ 0 & 0 & 0 & -(n/r) & -n & -(nz/r) & 0 & 0 & 1 \end{bmatrix} \begin{bmatrix} b_{1n} \\ b_{2n} \\ b_{3n} \\ b_{4n} \\ b_{5n} \\ b_{5n} \\ b_{7n} \\ b_{8n} \\ b_{9n} \end{bmatrix} \tag{29a}$$

or symbolically

$$[\epsilon_n] = [g_n][b_n] \tag{29b}$$

The evaluation of Eqs. (27) at the vertices i, j, and k results in an expression for the coefficient b_n in terms of the displacement amplitudes u_n:

$$\begin{bmatrix} b_{1n} & b_{4n} & b_{7n} \\ b_{2n} & b_{5n} & b_{8n} \\ b_{3n} & b_{6n} & b_{9n} \end{bmatrix} = [D] \begin{bmatrix} u_{rn}{}^i & u_{zn}{}^i & u_{\theta n}{}^i \\ u_{rn}{}^j & u_{zn}{}^j & i_{\theta n}{}^j \\ u_{rn}{}^k & u_{zn}{}^k & u_{\theta n}{}^k \end{bmatrix} \tag{30}$$

where $[D]$ is given by Eq. (15b). Equation (30) may be expanded to yield a column matrix of the nine constants b_n in terms of a column matrix of the nine displacement amplitudes u_n. Or in symbolic form

$$[b_n] = [h][u_n] \tag{31}$$

For a given stress-strain relationship, element stiffness matrices, Eq. (26a), and thermal load matrices, Eq. (26b), are evaluated for each element in the system. These matrices, for a given harmonic, are combined by direct stiffness techniques to obtain a relationship between unknown nodal circle displacement amplitudes and known nodal circle force amplitudes. The number of these two-dimensional problems, which must be solved, is determined by the number of harmonics which is required to represent the nonaxisymmetric loading.

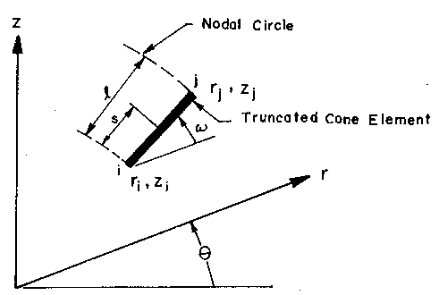

Fig. 4 Cross section of truncated cone element.

C. Quadrilateral Element

A typical quadrilateral element is composed of four triangular elements as illustrated in Fig. 3. For axisymmetric loads, the equilibrium equations for the quadrilateral are developed by standard direct stiffness techniques and involve ten equations, which are written in the following matrix form:

$$\begin{bmatrix} S_a \\ \hline S_b \end{bmatrix} = \begin{bmatrix} k_{aa} & \vert & k_{ab} \\ \hline k_{ba} & \vert & k_{bb} \end{bmatrix} \begin{bmatrix} u_a \\ \hline u_b \end{bmatrix} + \begin{bmatrix} L_a \\ \hline L_b \end{bmatrix} \tag{32}$$

where S_a, L_a, and u_a are associated with points 1–4, and S_b, L_b, and u_b are associated with point 5. Equation (32) may be written as two matrix equations, or

$$[S_a] = [k_{aa}][u_a] + [k_{ab}][u_b] + [L_a] \tag{33a}$$

$$[S_b] = [k_{ab}][u_a] + [k_{bb}][u_b] + [L_b] \tag{33b}$$

Equation (33b) may be solved for the displacements u_b:

$$[u_b] = -[k_{bb}]^{-1}[k_{ba}][u_a] + [k_{bb}]^{-1}\{[S_b] - [L_b]\} \tag{34}$$

If Eq. (34) is substituted into Eq. (33b), an expression is found relating the forces at points 1 to 4 to the unknown displacements at points 1 to 4 and the known loads

$$[S_a] = [\bar{k}_{aa}][u_a] + [\bar{L}_a] \tag{35}$$

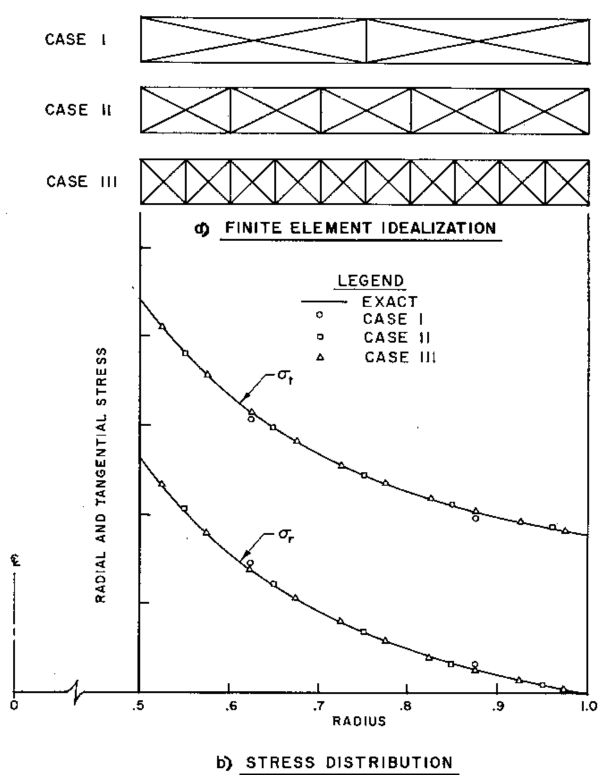

Fig. 5 Analysis of infinite cylinder.

where the quadrilateral stiffness matrix is

$$[\bar{k}_{aa}] = [k_{aa}] - [k_{ba}][k_{bb}]^{-1}[k_{ba}] \tag{36a}$$

and the modified thermal load matrix is

$$[\bar{L}_a] = [L_a] + [k_{ab}][k_{bb}]^{-1}[[S_b] - [L_b]] \tag{36b}$$

The use of the quadrilateral substructure as a separate element is desirable, since the resulting set of equilibrium equations has fewer unknowns for a given number of triangular elements. In the case of nonaxisymmetric loads, Eq. (32) would involve 15 equations relating force and displacement amplitudes and would reduce to 12 equations by a similar procedure.

D. Truncated Cone Element

In the stress analysis of thick sandwich shells, the orthotropic cone material is readily represented by solid triangular ring elements; and the face plates are idealized by a series of truncated cone elements, each connected at two nodal circles of the finite element system. The appropriate theory for the behavior of these axisymmetric shell elements subjected to nonaxisymmetric loading is given here. The cross section of a typical truncated cone element is shown in Fig. 4.

For the case of nonaxisymmetric loading, the displacements within the element are approximated by

$$u_r = \Sigma\,(b_{1n} + b_{2n}s)\cos n\theta \tag{37a}$$

$$u_z = \Sigma\,(b_{3n} + b_{4n}s)\cos n\theta \tag{37b}$$

$$u_\theta = \Sigma\,(b_{5n} + b_{6n}s)\sin n\theta \tag{37c}$$

The constants b_n are obtained by evaluating the displacements at the connecting nodal circles

$$\begin{bmatrix} b_{1n} & b_{3n} & b_{5n} \\ b_{2n} & b_{4n} & b_{6n} \end{bmatrix} = \begin{bmatrix} 1 & 0 \\ -(1/l) & 1/l \end{bmatrix} \begin{bmatrix} u_{rn}{}^{i} & u_{zn}{}^{i} & u_{\theta n}{}^{i} \\ u_{rn}{}^{j} & u_{zn}{}^{j} & u_{\theta n}{}^{j} \end{bmatrix} \tag{38a}$$

or expanded symbolically in column matrix form

$$[b_n] = [h]\,[u_n] \tag{38b}$$

The inplane displacement within the element is

$$u_s = u_r\cos\omega + u_z\sin\omega \tag{39}$$

The corresponding inplane strains are

$$\epsilon_{ss} = \Sigma\,\epsilon_{ssn}\cos n\theta = \partial u_s/\partial s \tag{40a}$$

$$\epsilon_{\theta\theta} = \Sigma\,\epsilon_{\theta\theta n}\cos n\theta = (1/r)(\partial u_\theta/\partial\theta) + (u_r/r) \tag{40b}$$

$$\epsilon_{s\theta} = \Sigma\,\epsilon_{\theta sn}\sin n\theta = (1/r)(\partial u_s/\partial\theta) + (\partial u_\theta/\partial s) \tag{40c}$$

Thus, the strain amplitudes may be evaluated as

$$\begin{bmatrix} \epsilon_{ssn} \\ \epsilon_{\theta\theta n} \\ \epsilon_{\theta sn} \end{bmatrix} = \begin{bmatrix} 0 & \cos\omega & 0 & \sin\omega & 0 & 0 \\ \dfrac{1}{r} & \dfrac{s}{r} & 0 & 0 & \dfrac{n}{r} & \dfrac{ns}{r} \\ -\dfrac{n}{r}\cos\omega & -\dfrac{ns}{r}\cos\omega & -\dfrac{ns}{r}\sin\omega & -\dfrac{ns}{r} & 0 & 1 \end{bmatrix} \begin{bmatrix} b_{1n} \\ b_{2n} \\ b_{3n} \\ b_{4n} \\ b_{5n} \\ b_{6n} \end{bmatrix} \tag{41a}$$

or symbolically

$$[\epsilon_n] = [g_n]\,[b_n] \tag{41b}$$

Therefore, for a given stress-strain relationship, the element stiffness matrix, Eq. (26a), and thermal load matrix, Eq. (26b), may be evaluated for a truncated cone element. The preceding equations reduce to the axisymmetric loading condition when n is zero.

IV. Application

Several digital computer programs have been developed for the finite element analysis of axisymmetric structures.

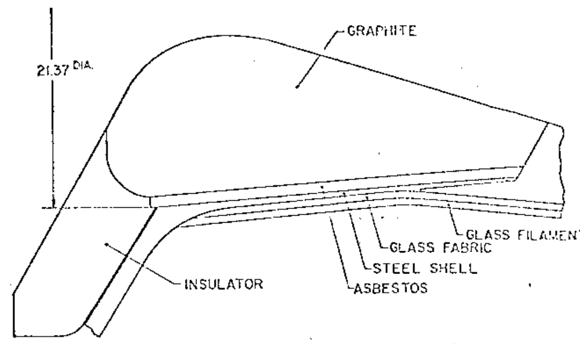

Fig. 6 Typical solid rocket nozzle.

The most general of these programs requires as input a complete numerical definition of all nodal circles and elements. Therefore, axisymmetric structures may be considered which are composed of many interacting components and are of practically any shape. In addition, special programs with built-in mesh generators have been developed for specific types of structures. The examples, that are presented here, are intended to demonstrate the validity of the method and to illustrate its application to complex structures.

A. Infinite Cylinder

An infinite cylinder subjected to an internal pressure for which an exact solution is known is selected as a means of demonstrating the accuracy of the finite element method. In Fig. 5a meshes for three finite element analyses are shown. The resulting radial and hoop stresses are plotted in Fig. 5b. Except for the very coarse mesh, agreement with the exact solution is excellent. Stresses are plotted at the center of the quadrilaterals and are obtained by averaging the stresses in the four connecting triangles. In general, good boundary stresses are estimated by plotting the interior stresses and extrapolating to the boundary. This type of engineering judgement is always necessary in evaluating results from a finite element analysis.

B. Rocket Nozzle

The typical rocket nozzle shown in Fig. 6 is selected to illustrate the application of the method to a complex axisymmetric structure subjected to axisymmetric thermal and pressure loading. The temperature distribution within the graphite insert at a specific time is plotted in Fig. 7. The element representation of the structure, as shown in Fig. 8, contains 501 elements and 280 nodal circles. The time necessary to select the mesh and prepare the computer input was approximately three man-days. The computer

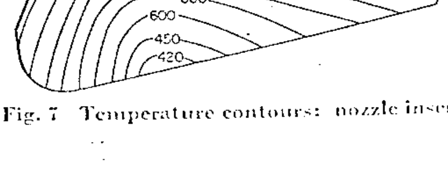

Fig. 7 Temperature contours: nozzle insert.

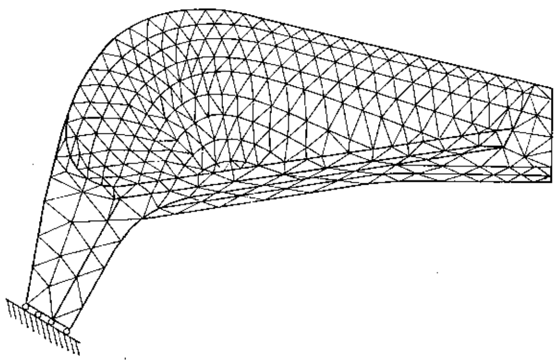

Fig. 8 Finite element idealization of nozzle.

time required by the IBM 7094 was three minutes. The computer program produces the four components of stress within each element and the two displacements of each nodal circle. Hoop stress contours are plotted in Fig. 9.

C. Spacecraft Heat Shield

A special program for the analysis of heat shields subjected to nonaxisymmetrical thermal loading has been developed. This program, which is based on the previously described method, automatically generates a mesh of quadrilateral ring elements, expands the temperature distribution into Fourier series and superimposes the harmonic solutions to obtain the displacements and stresses at desired points within the structure. A quadrilateral element representation of a typical heat shield is shown in Fig. 10a. In this case, the first two rows of elements represent a sandwich shell and the next four rows approximate the ablator. Truncated cone elements are used to represent the flanges of the sandwich shell. The temperature at the bond line between the ablator and shell is plotted in Fig. 10b. The temperature is constant through the shell and varies parabolically to a constant temperature at the surface of the ablator. Figure 10c illustrates typical results, displacement at the bond layer.

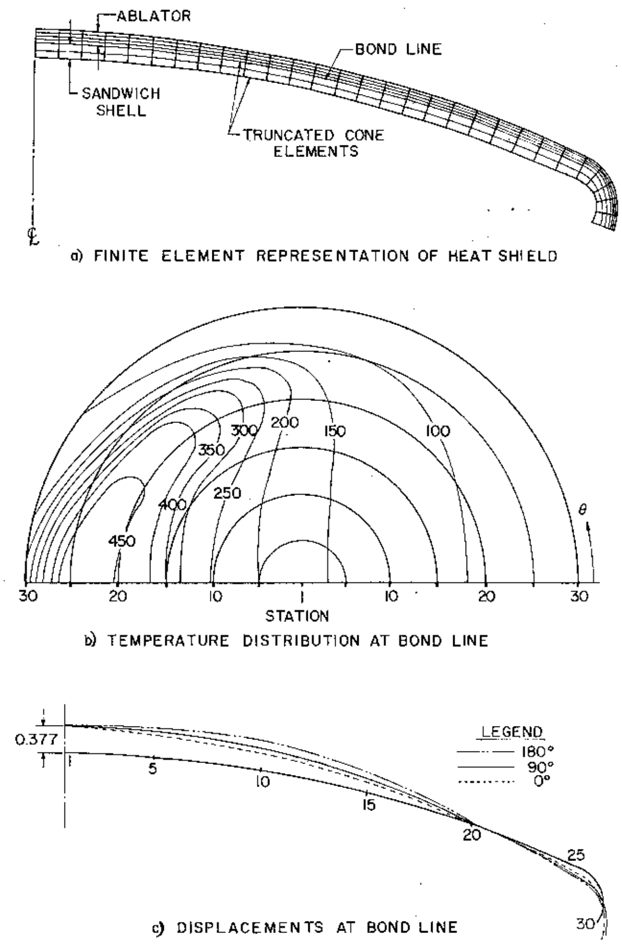

Fig. 10 Analysis of spacecraft heat shield.

V. Discussion

The finite element method has been applied to the determination of stresses and displacements within complex structures of revolution subjected to nonaxisymmetric thermal and mechanical loads. Since the method encompasses several classes of practical engineering structures, its importance as a tool in stress analysis is evident. With the aid of a computer program, the analysis of axisymmetric structures is reduced to a simple procedure that may be conducted without a detailed knowledge of the method or computer programing.

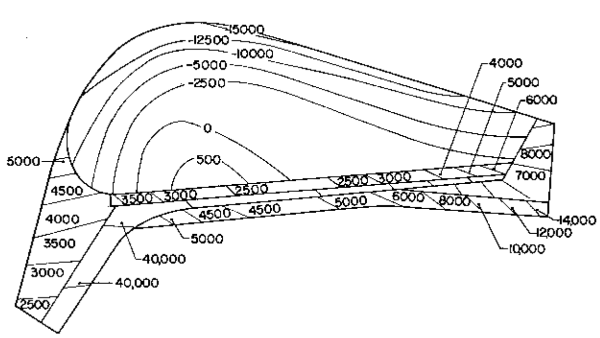

Fig. 9 Stress contours:hoop stresses.

References

[1] Argyris, J. H., *Energy Theorems and Structural Analysis* (Butterworths Scientific Publications, Ltd., London, 1960), Pt. I.

[2] Turner, M. J., Clough, R. W., Martin, H. C., and Topp, L. J., "Stiffness and deflection analysis of complex structures," J. Aeronaut. Sci. **23**, 805–823 (1956).

[3] Turner, M. J., Martin, H. C., and Weibel, R. C., "Further development and application of the stiffness method," *Matrix Method of Structural Analysis* (The Macmillan Company, New York, 1964), pp. 203–266.

[4] Grafton, P. E. and Strome, D. R., "Analysis of axisymmetric shells by the direct stiffness method," AIAA J. **1**, 2342–2347 (1963).

[5] Clough, R. W., "The finite element method in plane stress analysis," Proc. Am. Soc. Civil Engrs., 345–378 (1960).

[6] Gallagher, R. H., Padlog, J., and Bijlaard, P. P., "Stress analysis of heated complex shapes," ARS J. **32**, 700–707 (1962).

[7] Wilson, E. L., "Finite element analysis of two-dimensional structures," Structural Engineering Laboratory Rept. 63-2, Univ. of California, Berkeley, Calif. (June 1963).

[8] Clough, R. W. and Rashid, Y., "Finite element analysis of axi-symmetric solids," J. Eng. Mech. Div. **91**, 71–85 (1965).

[9] Melosh, R. J., "Basis for derivation of matrices for the direct stiffness method," AIAA J. **1**, 1631–1637 (1963).